

The Large Adaptive Reflector: A 200-m diameter, wideband, cm-m wave radio telescope

Brent Carlson^a, Luc Bauwens^b, Leonid Belostotski^c, Elizabeth Cannon^d, Ya-Ying Chang^e, Xiaohui Deng^b, Peter Dewdney^a, Joeleff Fitzsimmons^f, David Halliday^g, Kai Kürschner^e, Gerard Lachapelle^d, David Lo^g, Pedram Mousavi^h, Meyer Nahonⁱ, Lot Shafai^h, Sigfried F. Stiemer^e, Russell Taylor^j, Bruce Veidt^a

^aNational Research Council Canada, Herzberg Institute of Astrophysics, P.O. Box 248, Penticton, B.C. Canada V2A 6K3

^bDept. of Mech. Eng., Univ. of Calgary, 2500 University Dr. NW, Calgary, Alberta, Canada, T2N 1N4

^cDept. of Electrical & Computer Eng., Univ. of Alberta, Edmonton, Alberta, Canada, T6G 2G7

^dDept. of Geomatics, Univ. of Calgary, 2500 University Dr. NW, Calgary, Alberta, Canada, T2N 1N4

^eDept. of Civil Engineering, Faculty of Applied Science, Univ. of British Columbia, 2053-2324 Main Mall, Vancouver, B.C. Canada V6T 1Z4

^fNational Research Council Canada, Herzberg Institute of Astrophysics, 5071 Saanich Road West, Victoria, B.C. Canada V8X 4M6

^gAGRA Coast Limited, 1515 Kingsway Ave. Port Coquitlam, B.C. Canada V3C 1S2

^hDept. of Electrical & Computer Eng., Univ. of Manitoba, Winnipeg, Man., Canada, R3T 5V6

ⁱDept. of Mech. Engineering, Univ. of Victoria, P.O. Box 3055, Victoria, B.C. Canada V8W 3P6

^jDept. of Phys. & Astr., Univ. of Calgary, 2500 University Dr. NW, Calgary, Alberta, Canada, T2N 1N4

ABSTRACT

The Large Adaptive Reflector (LAR) is a concept for a low-cost, large aperture, wideband, radio telescope, designed to operate over the wavelength range from 2 m to 1.4 cm. It consists of a 200-m diameter actuated-surface parabolic reflector with a focal length of 500 m, mounted flat on the ground. The feed is held in place by a tension-structure, consisting of three or more tethers tensioned by the lift of a large, helium-filled aerostat—a stiff structure that effectively resists wind forces. The telescope is steered by simultaneously changing the lengths of the tethers with winches (thus the position of the feed) and by modifying the shape of the reflector. At all times the reflector configuration is that of an offset parabolic antenna, with the capability to point anywhere in the sky above $\sim 15^\circ$ Elevation Angle. At mid-range wavelengths, the feed is a multi-beam prime-focus phased array, about 5 m diameter; at meter wavelengths, it is a single-beam phased array of up to 10 m diameter. Simulations have shown that in operating wind conditions (10 m / s average speed with 2.5 m / s gusts), the position of the feed platform can be stabilized to within a few cm over time scales of ~ 20 s. Research indicates that the telescope concept is feasible and that an order of magnitude improvement in cost per m^2 of collecting area over traditional designs of large parabolic antennas can be achieved.

Keywords: radio telescope, phased array, reflector panel, space frame, actuator, aerostat, tether, parabolic, SKA.

1. INTRODUCTION

An international consortium of radio astronomers and engineers have agreed to investigate technologies to build the Square Kilometer Array (SKA), a cm-to-m wave radio telescope for the next generation of investigation into cosmic phenomena. A looming “sensitivity barrier” will prevent current telescopes from making much deeper inroads at these wavelengths, particularly in studies of the early universe. The aim of the SKA project is to increase the collecting area, the fundamental factor governing sensitivity, over existing telescopes by two orders of magnitude. The Large Adaptive Reflector (LAR) is a concept put forward by a group led by the National Research Council of Canada and supported by university and industry collaborators.^{1,2,3} The LAR concept is well suited to meeting the key SKA requirements of 150 MHz to 22 GHz operation, one square degree field of view at mid-range wavelengths, and sky coverage of about half the sky. So far, the LAR is the only future radio telescope concept that is being designed to operate from wavelengths of several meters to 1.4 cm.

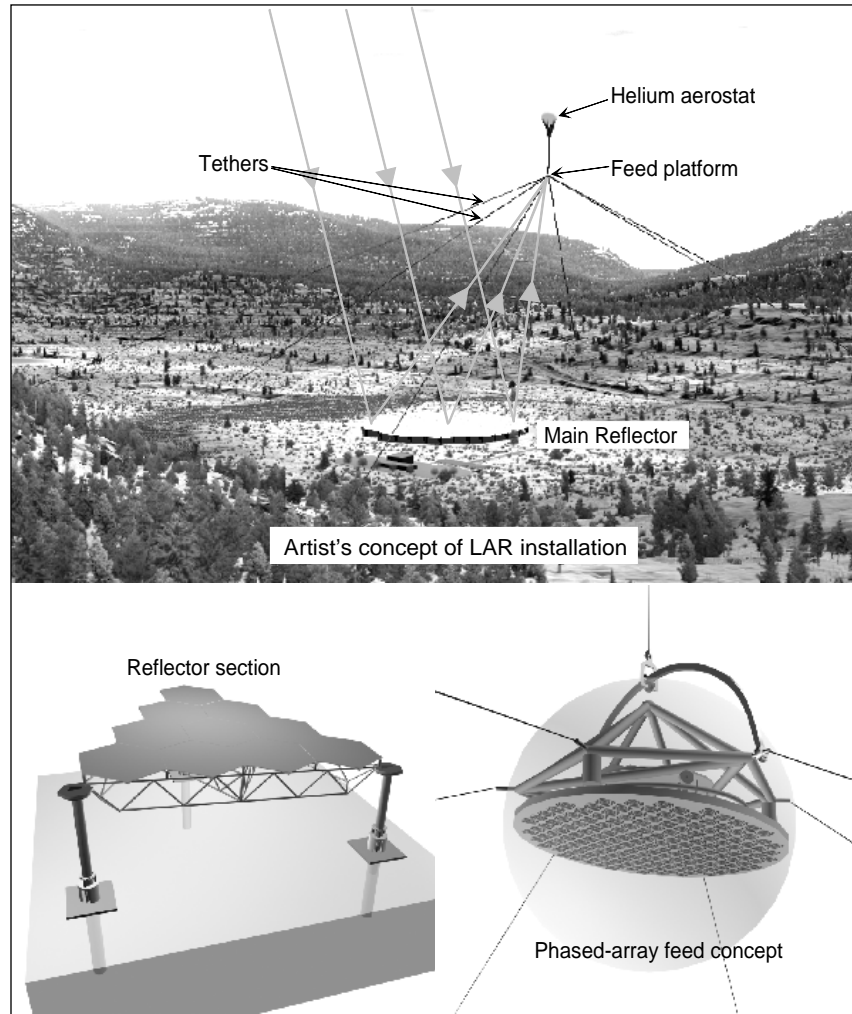


Figure 1 An artist's concept of a complete 200-m diameter LAR installation. The installation includes the main reflector, the multi-tethered aerostat system, the feed platform at focal length of 500 m, a surface measurement system (not shown) and a feed platform position measurement system (also not shown). Details of a main reflector section and the prime-focus phased-array feed concept are shown at the bottom of the figure. A full main reflector will contain about 150 sections. Each triangular section is supported by a space frame, and is 20 m on a side. Space frames are supported by large-stroke actuators that are shared with neighbouring space-frames. The phased-array feed contains pointing and stabilization mechanics, phasing networks, and cryogenic coolers. At 1.4 GHz, the feed is about 5.5 m in diameter and contains approximately 2700 elements which, along with the f/D ratio of 2.5, enables it to produce about 100 primary beams over approximately one square degree of sky.

Figure 1 is an artist's concept of an LAR installation with details showing a main reflector section and a phased-array feed concept. Before the SKA is constructed, a 200-m LAR prototype will be a powerful radio telescope in its own right with sensitivity and active collecting area on par with Arecibo but with wider frequency range, essentially all-sky coverage, and wide field-of-view. Research on the LAR in Canada has been broken into three basic phases. Phase-A, which has been completed, was a preliminary study to find reasonable (although perhaps not optimum) design solutions that would meet all of the requirements. The Phase-A study has been successful and has provided the research momentum to carry on to Phase-B. Phase-B is the alpha-prototype where critical (perhaps scaled) elements of the LAR are constructed and tested to determine if they will meet the design requirements. This phase is expected to take approximately 3 years to complete and is expected to begin in mid-2000. Pending the success of a critical review of Phase-B, Phase-C will be the construction of a full-scale, 200-m diameter prototype that will verify the operation of the LAR. Phase-C, including construction, development, and testing of operation at key frequencies is expected to take 5 to 7 years to complete. This paper will provide an overview of the results obtained in the Phase-A study. The elements of the LAR that will be covered include the actuated-surface main reflector, the main reflector surface-measurement system, the multi-tethered aerostat system, and the feed system (including the feed position measurement system and the precision focal distance measurement system).

2. THE MAIN REFLECTOR

The main reflector is a 200-m diameter actuated parabolic section. Its surface is actuated to maintain a shape equivalent to a standard offset parabolic antenna. As illustrated in Figure 2, it is essentially part of a much larger “virtual” parabola, which changes shape as the telescope is pointed in different directions (Zenith Angle and Azimuth). An approximate equation that governs the shape of the surface is

$$z = \frac{x^2 \cdot \cos(Za) + \frac{y^2}{\cos(Za)}}{4 \cdot R \cdot \left[1 + x \cdot \frac{\sin(Za)}{2 \cdot R} \right]}, \quad (1)$$

where z is the height of a point on the reflector surface and (x,y) is the projected position of that point on a horizontal surface under the reflector. The coordinate system rotates with Azimuth, the x -axis is in the plane of Figure 2, and the origin is at the projected center of the reflector. R is the distance from the centre of the reflector to the feed. Za is the Zenith Angle of the telescope’s pointing direction. $R = f$ at $Za = 0$, where f is the focal length of the paraboloid.

Note that this geometry provides an unblocked aperture, except near $Za = 0$. There are no scattering objects in the ray path from the sky to the focus (except occasionally one of the tethers, which will probably not have measurable scattering). The “clean optics” presented by this geometry will be helpful for making precise measurements and for rejecting sky-borne interference.

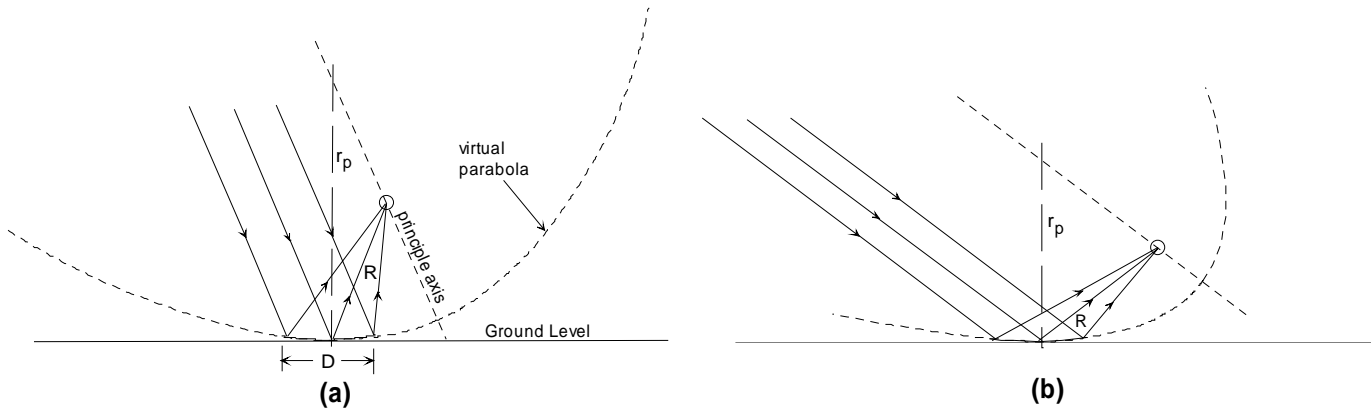


Figure 2 The LAR surface forms part of a much larger “virtual” parabola (shown in section along with its principle axis in dotted lines). For a fixed R , as Zenith Angle (Za) pointing changes, the height of the surface must only change a small amount along the x -axis (in the plane of the figure). Larger Za changes requiring larger actuator strokes occur along the y -axis (out of the plane of the figure) with increased zenith angle (b) since the radius of curvature (r_p in the figure) decreases. Note also that there is foreshortening of the available collecting surface area as Za increases. At $Za = 60^\circ$, the efficiency from foreshortening is 50% and at $Za = 75^\circ$, the efficiency is 26%.

The Phase-A study concluded that the optimum focal ratio at $Za = 0$ is about 2.5 ($R = 500$ m for a 200-m reflector diameter). This conclusion is based on a complex trade-off in an evaluation of many parameters, including feed stability, actuator throw, main reflector panel size, feed size, and footprint of the telescope installation. Of particular interest is the maximum actuator stroke, which occurs along the y -axis (out of the page in Figure 2). The required stroke for these parameters is about 7 m. An option for very large Zenith Angles is to permit the actuators to “saturate” at a particular height. An interesting feature of this possibility is that the loss of collecting area is very small, and it occurs on the reflector where it is least needed. In fact the beam on the sky becomes less elliptical at large Zenith Angles as a result of this effect.

2.1 Main Reflector Components

Cost is a major issue in designing the main reflector. Note that the cost per m^2 of surface will be much lower than for an equivalent standard parabolic reflector, where the entire reflector must be tilted to large angles. Here the cost per unit area does not increase quickly with diameter. There are many possible designs for constructing the reflector. The results of the Phase A study indicate the general approach described above for an LAR operating down to 1.4 cm. Large primary actuators

support triangular space frames that form the main structure of the surface. Reflector panels, proposed to be constructed of a low-density concrete composite, are supported by short stroke (10-15 cm) secondary actuators that provide final surface adjustment. The details are described in the following sections. Since the design of the reflector panels strongly influences the design of the support structure, they are described first.

2.1.1 Reflector Panels

The requirements for the reflector panels are that they are inexpensive, easy to construct, and stiff enough to meet the surface accuracy requirements for operation at a wavelength of 1.4 cm (rms surface accuracy of about 0.7 mm). Because of the long focal length, the panels can be fixed shape (nearly flat) and need not be particularly light, since they are all being supported directly by the ground. A concrete-and-steel construction ensures that wind-induced deflections will be negligible. A possible construction technique (Figure 3), which has been investigated in some detail⁴, is to construct the panels of steel-fiber reinforced concrete (SFRC) with an embedded steel frame. Once the panel has cured, the radio-reflecting surface, such as a spray-on, “self-healing” zinc coating, is applied. This design comes close to meeting the accuracy specifications, including thermal deformations. Figure 3 shows that the nominal rms is about twice that needed, but this is for a larger than expected front-to-back temperature gradient (10 K).

Although the panels do not have to be particularly light, the load of the concrete panels does, to a large extent, drive the cost of the backup structure and supporting actuators. As such, alternative designs and cost-effective materials for the panels are being considered with the goal of further reducing the cost of the main reflector structure.

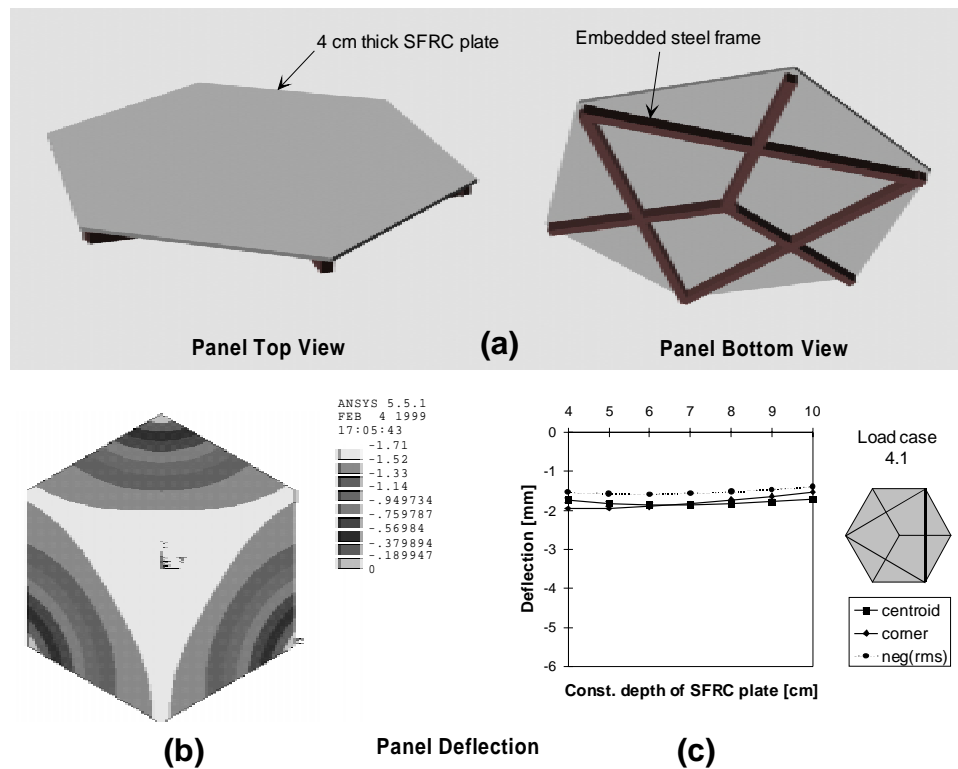


Figure 3 Steel fiber-reinforced concrete reflector panel design. Top and bottom views of the ~5 m diameter panel design are shown in (a). The embedded steel frame is 10 cm thick. In (b), the gravitational deflection of a 4-cm thick panel is shown. In (c) the thermal deflection for a 10 K thermal gradient (front-to-back) is shown for concrete plate thicknesses from 4 to 10 cm - at 4 cm, the RMS error is about 1.5 mm. Note that increasing the plate depth beyond 4 cm does not significantly improve the results. There will be about 1500 panels in a 200 m diameter main reflector.

2.1.2 Secondary (Short-Stroke) Actuator

The secondary actuators are short-stroke actuators whose job it is to provide fine surface adjustment on a panel-by-panel basis, and to compensate for short-term time variations that cannot be compensated for by the primary actuators (or possibly to compensate for non-linearity caused by the primary actuators). Secondary actuators will be shared (by adjacent panels) and positioned at the three corner-points under every panel. Currently, these actuators are envisioned to be ball-screw type electric actuators (perhaps with springs to reduce dead loading), although there is some consideration to use alternatives, such as fluid-filled bellows-type actuators. These devices find widespread use as air-springs in large trucks as well as air-actuators in harsh and difficult geometric conditions. They can be filled with fluid (anti-freeze) to increase their stiffness.

2.1.3 Triangular Space Frame

The triangular space frame forms the main structure onto which reflector panels are mounted. It must support the panels and maintain stability in windy conditions. The space frames are a major cost item in the reflector design and considerable effort has gone into minimizing the amount of steel used in their construction. If each triangular section of the reflector were an independent structure, then the trusses composing the sides of the triangles would run side-by-side for adjacent triangles. This redundant structure is removed in the current concept for the space frame design (Figure 4). Alternate triangles are replaced by bridging sections, and the amount of steel is reduced by a factor of about 1.7. Also in this design, secondary actuators can be attached to a single truss, although an expansion joint will be required where adjacent panels meet between sections.

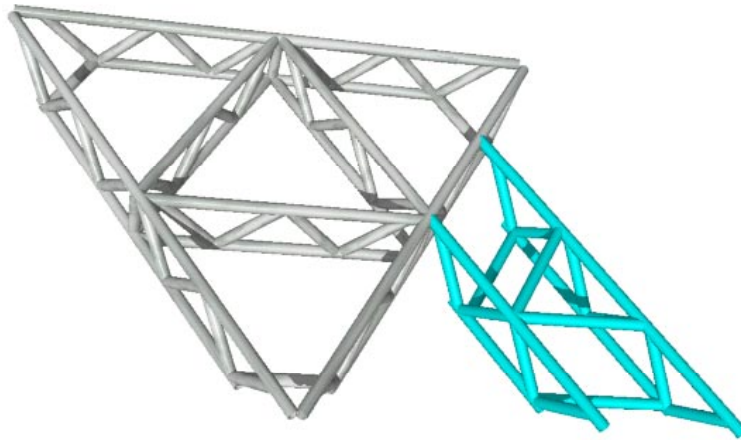


Figure 4 Triangular space frame design with bridging structure. The major triangular trusses (left of figure) form the foundation of the backup structure. They are about 20 m on a side. To avoid parallel trusses running side-by-side in adjacent space-frames, alternate space-frames in the overall structure are formed by using the bridging members (right of figure). This design meets backup structure requirements with a significant reduction in steel and cost.

2.1.4 Primary (Large-Stroke) Actuator

The primary actuator design is fundamental to the construction of the main reflector. In the 200-m LAR, there will be about 100 primary actuators that are used to support and vertically move the triangular space frames. The primary actuators need to be able to support a load of several tens of tons, they must be able to support an overturning moment, they must have a stroke of up to 7 m, they must be able to slew smoothly at low speeds, and they must be inexpensive (<~\$30k each). The maximum slew rate requirement is about 2.7 mm/s for slewing the surface over its whole range in about 1 hour. The maximum slew rate while tracking a radio source is less than 1 mm/sec. A concept that aims to meet the above criteria is shown in Figure 5(a). The principal motivation for this concept is to make the cost of the actuator independent of the actuator stroke, as much as possible. A relatively small volume of the actuator is required for the motive power and complex moving parts, whereas the pipe column can be extended as long as necessary. The pipe column is moved by alternately inserting the load pins into holes at intervals in the pipe and driving upper and lower hydraulic sections. The challenge of this design is to ensure that the hand-over from one hydraulic section to another occurs as smoothly as possible (although because of the low slew rate, short interruptions in motion while hand over occurs can be absorbed by the secondary actuators).

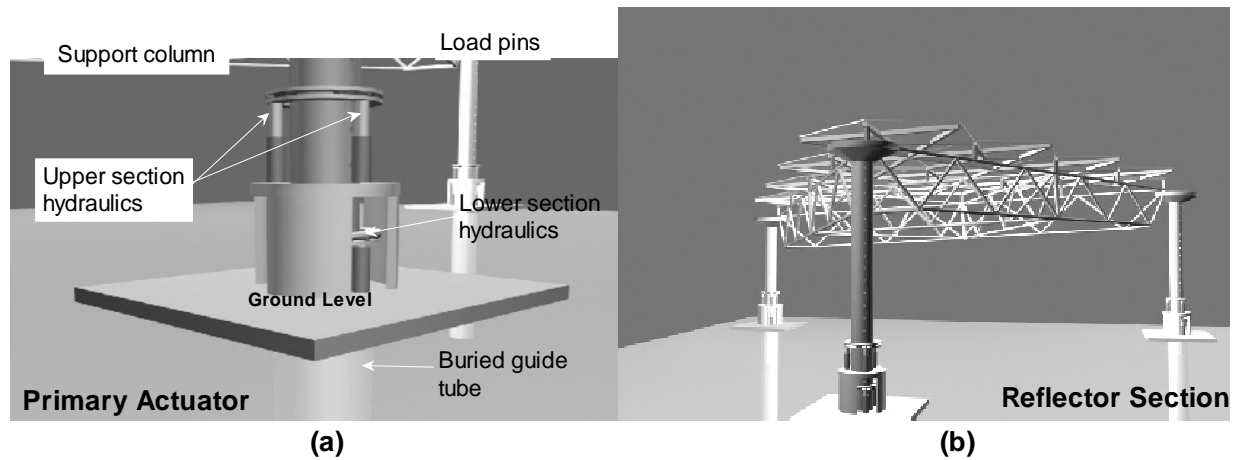


Figure 5 a) Details of the primary actuator. The actuator consists of a hollow steel pipe approximately 45 cm in diameter with 3 columns of holes in which load pins are inserted to support the pipe. The upper and lower sections contain 3 short-stroke (~30 cm) hydraulic actuators. The support column is moved by alternately engaging load pins and driving actuators in the upper and lower sections. The support column slides (with rollers not shown) into a buried guide tube in the ground. The column supports an overturning moment by ensuring that a minimum section of the support column stays in the guide tube even when fully extended. b) A triangular space frame with three supporting actuators. In the full surface, adjacent space frames will be supported by shared actuators requiring stretch/sliding joints between them. Reflector panels are supported by short-stroke secondary actuators mounted on the space frame. Panels are hexagonal in shape and approximately 5 m in diameter. Space frames are approximately 20 m in length along each of their sides, 2 m deep, with webbing constructed of 10 to 12 cm diameter steel pipe.

2.1.5 Expansion Joints: Steel-Rubber Bearings

As the surface changes shape with antenna pointing, the total surface area also changes. Thus, there must be some freedom in the joints where triangular space frames meet at primary actuators and where panels meet at secondary actuators. Vulcanized steel-rubber bearings of the type shown in Figure 6 will provide the appropriate movement. In addition, universal-joints are needed to provide rotational freedom at one vertex of the triangular space-frames. These bearings can sustain very large shear deflections with very little simultaneous vertical deflection under large vertical loads. As shown in Figure 6, they can be designed for movement in one or two-dimensions. These inexpensive devices are widely used in bridge structures for thermal expansion relief and in buildings for base-isolation from earthquake effects. They require no lubrication or maintenance, and are commercially available in a number of sizes and configurations.

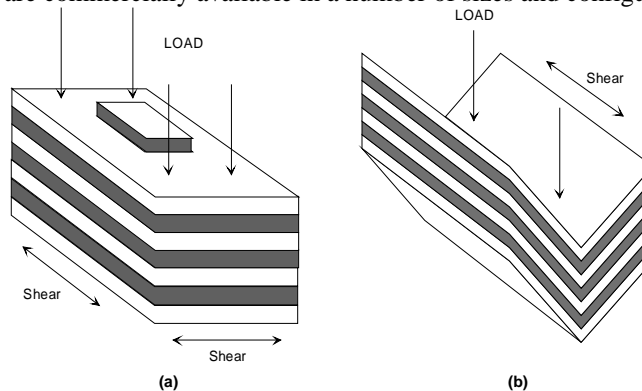


Figure 6 Steel-rubber bearings allow slippage in x and y axes (a) while still maintaining z-axis stiffness and stability. To constrain slippage to one lateral axis, a v-shape is employed (b). The shear slippage can be up to one-half the thickness of the sandwich of steel plates and vulcanized rubber. These bearings will be employed, along with universal joints, at the vertices of triangular space frames where they meet at primary actuators. Smaller versions of the bearings will be used where reflector panels meet at secondary actuators.

Calculations indicate that there will be a worst-case gap of about 15 cm between panels (obtained by tilting the primary actuators at about a 5° angle to the center of the dish) when they are at their maximum slope. These gaps do not pose a serious threat to the beam-shape, but they will cause an increase in the system temperature of the telescope if ground-radiation is permitted to propagate into the feed-antenna. A metal scattering interface is needed to block the ground radiation. This can be done by using a formed “under-lapping” metal lip along the bottom edge of the panels.

2.1.6 Surface Measurement System

Because the surface comprises independently actuated panels, the position of each panel must be measured, and the results provided to the control system that is responsible for setting the surface to the commanded shape. The surface measurement system provides this service as rapid (~1 per second) precision (~0.5 mm) measurements of the position and orientation of the panels. Because of the nearly flat geometry of the main reflector, it is not feasible to measure the surface from locations above the surface using optical or radio techniques. There are no convenient vantage points. Constructing vantage points that would provide good triangulation angles would be expensive and difficult, and could produce aperture blockage. Additionally, above-surface multiplexed measuring schemes cannot measure the roughly 1500 panels quickly enough to track their motion while observing. Thus, the surface must be measured using devices positioned on the ground, below the surface.

Three possible methods are currently envisioned. The first is short-range photogrammetry using inexpensive black-and-white video cameras. A possible geometry for this using a single camera system is shown in Figure 7. However, a three-camera system may be required in practice to compensate for target location and camera focal length instabilities. Moreover, this method may have environmental problems associated with dust-collection on lenses, moisture and insects, although these problems can likely be overcome by taking appropriate design precautions.

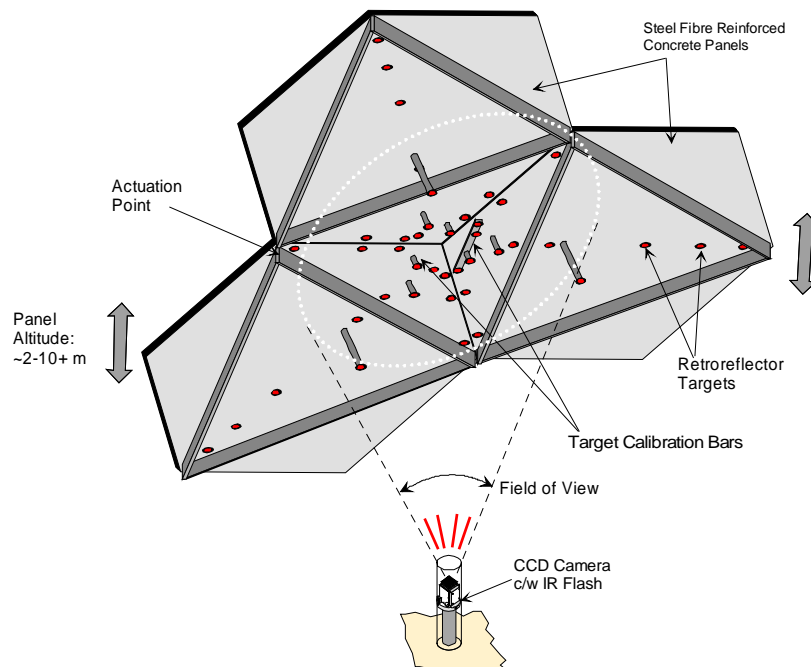


Figure 7 Single-camera, short-range photogrammetry system. A camera mounted on the ground takes pictures of infrared-illuminated retro-reflective targets on the backs of the panels. Given the geometry of camera lens and the optical sensor (a charge-coupled device (CCD)), and knowing the separation between targets on the panels, the x, y, and z coordinates of the targets within the camera's field of view can be determined. Simulations indicate that a single-camera system may provide sufficient accuracy provided the camera focal-length is stable with temperature (or can be temperature compensated). A temperature-stable "calibration bar" must be mounted on the panel to compensate for thermal expansion of the panel. With a single-camera measurement system, about 400 cameras are required to measure the surface. If a multi-camera system is required (in which case target separations and camera focal lengths need not be known) then about 1200 cameras will be required.

A second measurement method uses time-of-flight laser ranging at several sites under the surface to measure the distance from the ground to retro-reflective control surfaces on the back of each panel. This method is illustrated in Figure 8. The laser is directed by a mirror rotating about the z-axis and by mirrors mounted at known positions on the ground to targets on

the panels. The mirror-mount on the ground contains three or more mirrors that direct the laser beam to a location on each of three panels where they meet at an actuator, thus providing the fundamental information needed to provide their position and orientation. Depending on how this method is used, large areas of reflective material to account for motion of the panel may be needed. The mirror-mount also contains a retro-reflector so that absolute calibration of the time of flight can be performed. The speed (and therefore the number of panels that can be measured with each laser) with which measurements can be made will be determined by the bandwidth of the laser modulation and how fast the beam-steering mirror can be positioned. If the beam-steering mirror can be freewheeling (i.e. not have to step to certain locations) then measurements can be obtained from many panels in one sweep (provided the signal-to-noise ratio/bandwidth is high enough). Additionally, each laser will occasionally measure the distance to LAR perimeter retro-reflectors that form the foundation of the LAR coordinate system—thus determining the position and attitude of the laser on an on-going basis.

The third method is a variation of the second method whereby there is a time-of-flight laser mounted on the ground underneath each panel. This laser simply determines the z distance to the overhead panel—x and y coordinates are determined by virtue of the location of the laser on the ground. This method is potentially the simplest method since no mechanical moving parts are involved and each panel can be measured very rapidly. However, due to the large number of devices required (about 1500), this method is attractive only if a precision time-of-flight laser device can be manufactured or purchased for less than about \$2000.

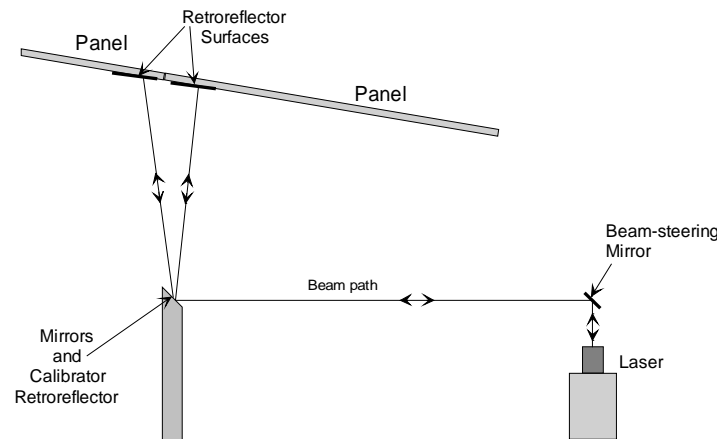


Figure 8 A second possible surface measurement method. A time-of-flight laser, steered by a mirror with z-axis rotation, first measures the distance to the panels with mirrors via the path shown. It then measures the fixed distance to a calibrator retro-reflector adjacent to the mirrors that provides continuous absolute calibration. Additionally, it will occasionally measure the distance to LAR perimeter retro-reflectors that form the foundation of the LAR coordinate system. The rate at which panels can be measured will be determined by the rate at which the beam-steering mirror can be re-pointed and by the bandwidth of the laser modulation.

3. THE MULTI-TETHERED AEROSTAT SYSTEM

The key element of the LAR that makes it possible to build such a large offset paraboloid is its long focal length (about 500 m). This focal length and the desire to point the telescope to Zenith Angles as high as 75° at all Azimuths rules out a rigid member structure to support the feed. Instead a tension-structure is employed, similar to the guyed structures used for antenna masts and similar structures. The principle of a tension-structure is that there is sufficient tension force in the tethers to offset external horizontal forces, wind in this case (i.e. the tethers are “pre-tensioned”). Wind-induced deflections are small if there is sufficient tension that deflection forces do not significantly change the profile of the tethers, but rather stretch the tethers instead. In the case of the LAR, an aerostat provides a lifting force sufficient to maintain tension in the tethers during the worst-case operating conditions, as well as to carry the load of the feed platform. A critical element of the success of this structure is the strength-to-weight ratio of the tether material. Strong, light cables made of such materials as Kevlar and Spectra, which have eight times the strength-to-weight ratio of steel cable, are commercially available. Reasonably priced aerostats are also commercially available with the net lifts required (about 40 kN) for this application. Referring to Figure 1, the tethered system contains several components: the tethers, the feed platform, the winches, the aerostat, and a control system (to drive the winches). The control system must maintain the feed platform, which is located at the confluence point of the tethers, at the focus of the reflector. The aerostat is offset from the confluence point by a “leash”, which is about 100

m long. The leash acts as a mechanical low-pass filter that minimizes the coupling of motion of the aerostat to the feed platform. The minimum number of tethers is three. However, six tethers have been found to reduce the footprint of the telescope, to improve Azimuth pointing and to increase slightly the open-loop stability of the system.

The stability of the feed/confluence point is fundamental to the feasibility of the LAR. As such, extensive work has been done to model the dynamical motion of the confluence point in gusty wind conditions. The model's computer code has its heritage in the computer simulation of towed robotic undersea vehicles, where it has undergone extensive experimental validation.

A particularly important issue is the selection of the type of aerostat. A spherical aerostat suffers about five times greater deflection in the wind than a streamlined aerostat. Moreover, a spherical aerostat is subject to alternating vortex shedding from its the surface. (This effect is not currently modeled.) However, there is an impetus to study a spherical aerostat for the LAR, since a streamlined aerostat requires more complex (expensive) ground-handling equipment. Research reports from this field indicate that spherical aerostats can be modified to reduce vortex shedding.

Figure 9 shows early simulation results from a three-tether LAR system. The simulated system utilizes a 20-m diameter, spherical aerostat. The computer model has recently been enhanced to include a streamlined aerostat, six tethers, and more advanced control system. These changes should result in improved performance over that indicated in Figure 9.

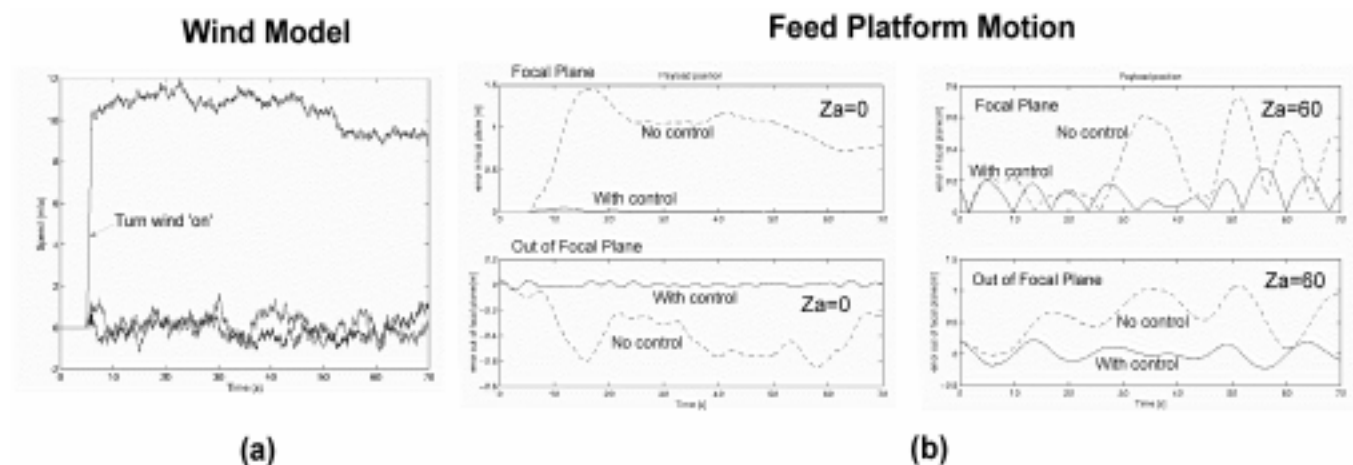


Figure 9 Dynamic simulation of the motion of the confluence point (feed platform). The wind model (a) is two-dimensional in the sense that it has the same forcing function at every point along its entire “front”. Once “turned on”, the wind model has a average speed of 10 m/s with about 2 m/s wind gusts. The top trace is the direction of the wind (x-axis) and the bottom traces are orthogonal to the main direction of the wind. The motion of the feed platform/confluence point (b) with and without a tether control system is shown in the $Z_a = 0^\circ$ and $Z_a = 60^\circ$ cases. The control system employed is a simple “proportional integral derivative” (PID) system. Without control, the feed platform moves about 50 cm in the wind on time scales of 10-20 seconds. With control, its motion is reduced to a few cm. Final feed platform stability will be achieved on the feed platform itself.

3.1 Position Measurement

The system that controls the position of the feed must have measured 3-D position information. The accuracy of this measurement will control how well the antenna can be pointed. We propose to use differential GPS (Global Positioning System) methods, combined with the high-precision focal distance measurement described in Section 5. Differential GPS is a standard technique that has been highly refined for this case. The essence of the technique is that GPS receivers are located both in known, fixed positions on the ground and on the moving feed platform, all receiving signals from the same satellites. Differential analysis of the results permits the cancellation of atmospheric propagation and selective availability effects to yield high precision results. A minimum of three GPS receivers are also mounted on the non-mechanically stabilized portion of the feed platform* to determine its attitude and position. The measurements from the ground GPS receivers, the feed

* The GPS receivers primarily measure the position of the feed platform structure to provide uncompensated location information for the tether control system. Local measuring devices will then determine the position of the stabilized feed portion relative to the platform structure.

platform receivers, and the focal distance measurement system are then combined to yield the position and orientation of the feed platform. The results of recent studies indicate that sub-cm measurement accuracy can be achieved. This is close to the 3.5 mm requirement for operation at a wavelength of 1.4 cm. GPS techniques are inexpensive and highly developed. However, there are several alternatives if GPS is not suitable. A method is described in Section 5 for accurately measuring the straight-line distance to the feed platform. Three of these would provide the 3-D position. The orientation of the feed platform can then be measured with commercially available inclinometers.

3.2 Mechanical Stabilization of the Feed

The feed must be stabilized to an accuracy of $\pm\lambda/4$ (for a focal ratio of 2.5) in the focal plane to maintain accurate pointing of the telescope to $1/10^{\text{th}}$ of its primary beam. Orthogonal to the focal plane, the stabilization requirements are much less severe (about 5 m at 1.4 GHz), due to the large depth-of-field of the telescope. At a wavelength of 20 cm (1.4 GHz), the focal plane stabilization requirement is about 5 cm; at a wavelength of 2 m (150 MHz), it is 50 cm; at 1.4 cm (22 GHz), it is about 3.5 mm. The following factors are important in considering this problem: a) The stability requirement scales with the size of the feed. At low frequencies where the feed is largest (and the most difficult to stabilize), the stability requirement is least stringent and at the highest frequencies where the feed is smallest (and inherently the easiest to stabilize), the stability requirement is most stringent. This relation assists the effort to adequately stabilize the feed over the entire range of observing frequencies. b) A stabilizer need only remove the high frequency velocity components of the feed motion—any slowly varying offsets (or constant offsets) can be tracked by imparting a tilt component to the shape of the main reflector. Since the reflector is fully actuated, this does not require additional equipment. c) An inertial stabilization system could be used. Such a system need not require much actuator power, since no force is needed to keep a mass from moving. A modified Stewart platform is envisioned that stabilizes the feed in translation, attitude, and rotation about the principle axis of the feed. Since the tethers can be used to provide most of the orientation motion of the feed and the residual errors in position (translation) will be small, the ranges of motion required of the stabilization system are quite small. A mechanical stabilization system may not be needed at wavelengths longer than about 20 cm.

4. THE FEED

Because the LAR uses reflective optics, its inherent frequency range is limited at the short wavelength extreme by errors from the faceted approximation to a parabolic surface and panel surface accuracy, and at the long wavelength extreme by the maximum dimensions of the feed. The design goal is to cover the wavelength range from 2 m to 1.4 cm (easily covering the SKA goal) using a number of feed packages, each with approximately octave bands. The SKA also requires a field-of-view of about 1 square degree at a wavelength of 20 cm. Since an individual beam is much smaller than 1 degree, this requirement can only be met with a multi-beam feed. The LAR's long focal length ensures that off-axis beam-distortions will be minimal. Thus the main challenge is to illuminate the reflector with enough beams to cover the field-of-view (about 100 at $\lambda = 20$ cm), and to be able to adjust the illumination patterns of the beams to compensate for the $\cos(Z_a)$ foreshortening effect.

Table 1 Antenna Performance of the LAR at Meter Wavelengths (10 m feed)				
Frequency (MHz)		75	150	300
T_{gal} (K)		1400	200	35
$Z_a = 0^\circ$	$\eta_{\text{spill}}^{\text{a}}$	0.64	0.93	0.98
	T_{ant} (K) ^b	1000	210	40
	θ_{beam} (deg)	69	34	17
$Z_a = 60^\circ$	η_{spill}	0.34	0.84	0.96
	T_{ant} (K)	670	220	5
	θ_{beam} (deg)	137	69	34

$$^{\text{a}} \eta_{\text{spill}} = \frac{\Omega_{\text{spill}}}{\Omega_{\text{main}} + \Omega_{\text{spill}}}$$

$$^{\text{b}} T_{\text{ant}} = \frac{T_{\text{gal}} \times \Omega_{\text{main}} + 300 \times \Omega_{\text{spill}}}{\Omega_{\text{main}} + \Omega_{\text{spill}}}$$

can be made to work successfully for a single, on-axis beam. This could be useful for deep space and transmitting applications. However, implementing multiple beams would require an impracticably large separation of feeds on the ground, because of the extremely large magnification of the Cassegrain configuration.

The multi-beam, variable shape feed patterns dictate a phased-array approach to the problem at decimeter and cm wavelengths. Several configurations have been investigated, including some for which additional reflector elements are introduced into the optical path. A feed on the ground, used in conjunction with a sub-reflector at the prime focus (similar to a Cassegrain configuration)

At longer wavelengths, the field-of-view is large enough with only a few beams. The feeds can be thin, wire-like structures, much less dense than needed at short wavelengths. Furthermore, the required position accuracy of the feed platform is inversely proportional to wavelength. Thus a feed structure of order 10 m in diameter is envisioned at m wavelengths. Table 1 contains estimates of the efficiency, and spillover plus sky noise contributions to the system temperature at meter wavelengths⁵.

4.1 Prime-Focus Phased-Array Feed

Fundamental considerations: So far, phased-array feeds centered near a wavelength of 20 cm, the mid-frequency range of the telescope, have been studied in some detail. A phased-array feed consists of three fundamental “layers”. First, there is the array, itself, composed of small (low gain) antenna elements, spaced closely together, probably in a hexagonal array on a plane. Directly behind this plane is an array of receivers. Beyond the receivers in the signal path is a combining network that combines the signals from the receivers to produce the required number of beams on the sky. Each beam will result from the combination of signals from a sub-array of proximate elements. The important design decisions are: a) choose mechanical or electronic steering for pointing of the reflector for different Zenith Angles, b) choose an element spacing, c) choose a type of array element.

Mechanical steering has advantages: a) A large fraction of the mechanical steering angle occurs “naturally” as the tensions of the tethers are adjusted for various Zenith Angles, b) no phase shifters or delay elements are needed in the combining networks, c) the size of the array is minimum because foreshortening at large “look angles” is avoided, d) an element spacing of 1λ instead of 0.5λ is sufficient to avoid grating responses, e) there are no blind spots or other artifacts of electronic steering over large angles.

It is important to maximize the bandwidth of the feed so as to minimize the number of focal packages that must be produced. The bandwidth is limited more by the properties of the array than (say) by the properties of the individual array elements. As noted above, the element spacing at the short wavelength end must be slightly less than 1λ to avoid a grating lobe in the plane of the array that would receive signals, including ground noise, near the horizon. This spacing is large enough to permit a variety of element-designs to be used, whose bandwidth is at least an octave. For example, Sinuous or Vivaldi elements will suffice.

The size of the main reflector focal-region (the “spot size”) is $(f/D)\lambda$. The spot must be properly sampled by the array of elements, and in this case the spot is larger than element spacing – thus the signals from a number of elements must be combined in a weighted sum to produce one beam on the sky. The actual number is wavelength dependent. In other words, to avoid under-illumination of the reflector at the short wavelength end, or spillover at the long wavelength end of the band the number of elements summed in the combining network must be scaled with wavelength. This is a significant effect over an octave band, and indicates that the band will have to be “channelized” into sub-bands before they can be combined.

Implementation: It is clear that losses in transmission lines dictate a receiver for each element. Receivers for wavelengths shorter than about 20 cm will have to be cooled to liquid nitrogen temperatures. The size of the system, the number of interconnections, and the required signal processing strongly indicate a digital approach to the combining network. We envision the signal processing steps to go as follows: a) digitize the signal from each receiver, b) digitally filter the signal into sub-bands, c) distribute the sub-band outputs to all the summing networks that require the signal as input, d) form the weighted averages needed to make beams. At 20-cm wavelength, the feed will be about 5.5 m in diameter with an array of about 2,700 antennas and receivers, whose signals will be combined to form about 100 beams. The feed elements will be simple elements that can be etched on a substrate. The challenges ahead are to build small receivers that can be cooled via distributions of liquid nitrogen, to distribute a Local Oscillator, and to construct a digital combining system that is sufficiently small and power-efficient to be included on the focal package. Recent progress in anti-aliasing techniques will permit the use of digital filtering methods without resorting to heavy, expensive RF anti-aliasing filters. The mass target for the entire focal package is 1000 kg, sufficiently small to leave plenty of “excess” lift for tensioning the tethers. Additional work on light, inexpensive liquid Nitrogen generators is also part of the focal package development project.

5. Focal Distance Measurement and Local Oscillator Delivery

Feeds in most parabolic reflector designs are fixed by “feed-legs” whereas the distance between the reflector and the LAR feed is not rigidly fixed. Thus when the LAR is used as an element of an interferometer, this distance must be measured and incorporated into the interferometer’s path-length compensator. Also, since receivers are located at the focus, a phase-stable

Local Oscillator (or more generally, a phase-stable reference signal) must be delivered to the focus. Figure 10 illustrates how a system based on a “round-trip” method (e.g.⁶) can be modified to operate over a radio link. Carrier frequencies are above the observing band. Modulation of the carrier by low frequencies provides frequency-division separation of the transmissions in the two directions. The phase of the signal, F_0 , entering the ground unit from the down-converter, contains the round-trip phase. This phase is halved in the ground unit, and then fed back to compensate for changes in length. This system cannot measure the absolute distance because of ambiguities, equal to the number of carrier wavelengths in the path. The ambiguities can be resolved by using several frequencies and their modulation products as shown in Figure 10. The slightly different numbers of wavelengths in the path for each carrier signal is analyzed using a variation of the Chinese Remainder Theorem to find the distance. A proof-of-concept model of this system has been built and tested at lower carrier frequencies than would be used for the actual LAR⁷.

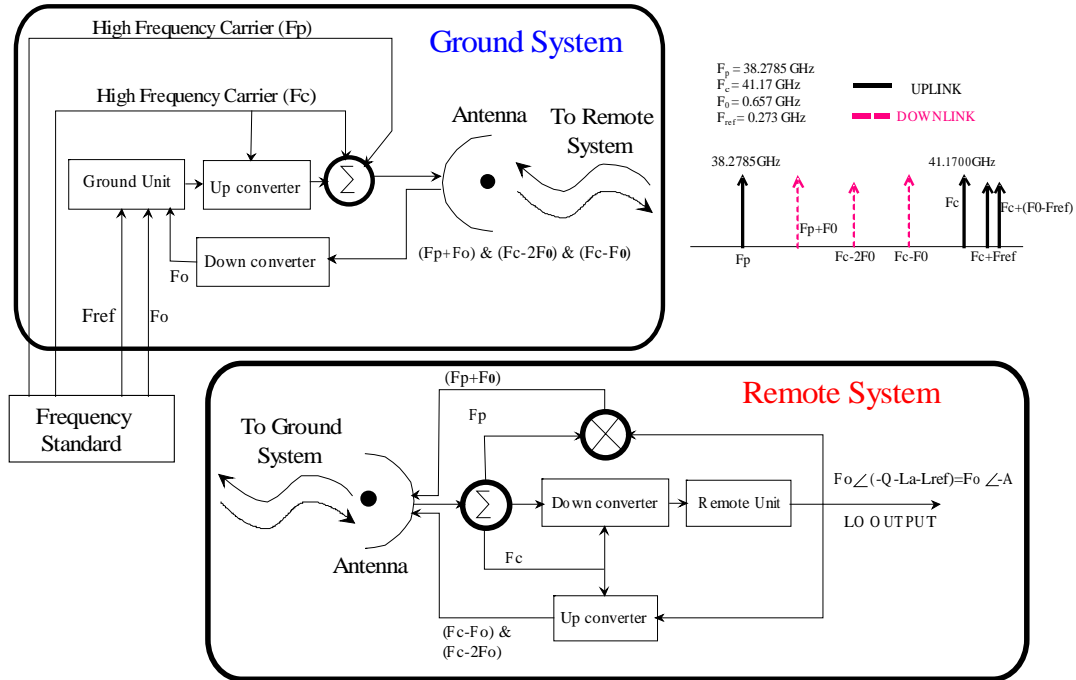


Figure 10 A “round-trip” system for continuously compensating for changes in the electrical length between reference points at the center of the LAR reflector, and on the feed antenna. The system utilizes multiple frequencies to deliver a Local Oscillator to the remote unit on the feed, whose phase is independent of the distance between the two reference points. In addition, it will measure the electrical length to within a small fraction of a cycle of the High Frequency Carrier without ambiguities.

ACKNOWLEDGMENTS

The funding for the Phase-A research presented was provided by a grant from the National Research Council of Canada.

REFERENCES

1. P. E. Dewdney & B.G. Veidt, “The Development of the Large Adaptive Reflector for the Square Kilometer Array – Specifications and Guidelines for Research”, *Report of the National Research Council of Canada*, 1997.
2. P. E. Dewdney, B.G. Veidt & B. R. Carlson, “The Large Adaptive Reflector – A Wide Band Radio Telescope Design”, *XXVI General Assembly of the International Union of Radio Sciences*, **Paper JBC.4**, Toronto, Aug. 1999.
3. T. H. Legg, “A Proposed New Design for a Large Radio Telescope”, *Astr. & Astro. Suppl.*, **130**, pp. 369-379, 1998.
4. K. Kürschner, “Conceptual Design of the Large Adaptive Reflector Panel for the Square Kilometer Array”
5. B.G. Veidt & P. E. Dewdney, “The Large Adaptive Reflector as an Efficient Decametric Antenna”, *XXVI General Assembly of the International Union of Radio Sciences*, **Paper JBC.5**, Toronto, Aug. 1999.
6. T. L. Landecker & F. Vaneldik, “A phase-stabilized Local-Oscillator System for a Synthesis Radio Telescope”, *IEEE Trans. on Inst. & Measurement*, **IM-31**, pp. 185-192, 1982.
7. L. Belostotski, “Local Oscillator and Focal Distance Measurement System for the Square Kilometer Array”, Thesis, University of Alberta, Dept. of Electrical and Computer Engineering, 2000.